Bending Tolerance of react&wind Nb_3Sn Conductors for Fusion Magnets

Pierluigi Bruzzone, Hugues Bajas, Chiara Frittitta, Federica Demattè, Kamil Sedlak, Xabier Sarasola, Valentina Corato

Abstract—**The react-and-wind technique for manufacturing of large Nb_3Sn fusion magnets (RW) is very attractive because of the superior performance of the Nb_3Sn with lower thermal strain compared to the wind-and-react technique. The procedure for magnet winding is also drastically simplified for the RW approach.**

The flat cable, made of a large number of Nb_3Sn strands, is heat treated on a spool with constant radius. Then the cable is unspooled to assemble the conductor with stabilizer/steel jacket and wound on a spool to be shipped to the winding factory, where the conductor is unspooled and wound in the final geometry – either round shape for Central Solenoid or D-shape for Toroidal Field Coils. The bending strain must be controlled during the handling from heat treatment to the final magnet in order not to exceed the irreversible strain. For design purposes, it is assumed so far that a bending strain ±0.3% during handling is acceptable.

In this work, the bending tolerance of a 63 kA RW fusion conductor is investigated by monitoring the performance in the SULTAN test facility after bending/straightening at decreasing radii till a degradation of the current sharing temperature performance, T_{cs}, is observed. The experimental assessment of the bending tolerance during handling is a major instrument for dimensioning of the cable thickness and heat treatment radius of the RW conductors for fusion.

Index Terms— **React-and-wind, Fusion Magnets, Bending strain,**

I. INTRODUCTION

THE Nb_3Sn intermetallic superconductor is the favorite material for magnets with peak field in the range of 8 T to 18 T. The brittleness (limited elastic range for deformation) and the strain sensitivity of the critical current density, J_c, call for dedicated measures at conductor handling and coil winding. The "wind&react", WR, method for manufacturing of Nb_3Sn based magnets is widely used for small winding radius, e.g. high field solenoids for laboratory and dipoles/quadrupoles for accelerators: the heat treatment to build the Nb_3Sn phase is carried out after winding the coil in the final shape. When the winding radius is large, both the WR and the "react&wind", RW, methods can be applied: in the RW approach, the Nb_3Sn cable is first heat treated on a round former and then it is unwound and assembled with the other conductor components, e.g. steel conduit, stabilizer and cooling pipe.

The J_c is higher in the RW method because the thermal strain of Nb_3Sn is smaller (range of -0.3%), with the steel added after heat treatment. In comparison, the thermal strain in WR is in the range of -0.6%. The ratio of J_c in RW and WR is about 2. The coil winding is by far cheaper for RW, skipping the complex procedure for electrical insulation needed for WR. For a discussion of the WR vs. RW approaches for Nb_3Sn fusion magnets see [1-2].

In the last two decades, the WR method dominates the Nb_3Sn fusion magnets, e.g. ITER [3], KSTAR [4] and JT60SA [5]. Relevant applications of the RW in fusion devices and facilities are MFTF [6], T-15 [7], SULTAN [8], DPC-EX [9], TRIAM [10] and LDX [11].

At the Swiss Plasma Center, SPC, of the EPFL, the RW method has been developed since 2014 for the high current superconductors of the EUROfusion DEMO magnets [12-15]. A key engineering parameter for design of RW magnets is the bending tolerance of the Nb_3Sn cable during handling: between the heat treatment and the final winding, the cable is unspooled (infinite bending radius) for jacketing, bent on spools for transportation (typical radius ≤ 2m) and eventually wound in the magnet. It is a requirement that the cable bending during handling does not cause irreversible performance degradation, i.e. the Nb_3Sn remains in the elastic range of deformation. The initial design assumption [1] is that bending strain in the cable up to ±0.3% is not causing any irreversible damage. In this work, the bending tolerance of a large size RW conductor is experimentally assessed by monitoring the current sharing temperature, T_{cs}, at 63 kA / 11 T after bending/straightening the conductor at decreasing bending radius.

Submitted for review September 19, 2023

This work has been carried out within the framework of the EUROfusion Consortium, partially funded by the European Union via the Euratom Research and Training Programme (Grant Agreement No 101052200 — EUROfusion). The Swiss contribution to this work has been funded by the Swiss State Secretariat for Education, Research and Innovation (SERI). Views and opinions expressed are however those of the author(s) only and do not necessarily reflect those of the European Union, the European Commission or SERI. Neither the European Union nor the European Commission nor SERI can be held responsible for them.

Pierluigi Bruzzone, Hugues Bajas, Chiara Frittitta, Federica Demattè, Kamil Sedlak and Xabier Sarasola are with EPFL-SPC, 5232 Villigen PSI, Switzerland (email: pierluigi.bruzzone@psi.ch, hugues.bajas@psi.ch, frittittachiara85@gmail.com, federica.dematte@psi.ch, kamil.sedlak@psi.ch, xabier.sarasola@psi.ch)

Valentina Corato is with ENEA, 00044 Frascati, Italy (email: valentina.corato@enea.it)

TABLE I
CONDUCTOR LAYOUT AND OPERATION DATA

Operating Current, kA	63.3
SULTAN Background Field, T	10.9
Peak Operating Field, T	12.23
Jacketed conductor size, mm x mm	61.5 × 32.1
Strand Diameter, mm	1.2
Cable Layout	(1 Cu +6+12) x 13
Cable pitches, mm	+105 / +390
SC cable size, mm x mm	35 × 10.8
Void fraction in cable	≈ 23%
J_{copper}, A/mm^2	90
$J_{non\text{-}copper}$, A/mm^2	478
Central steel strip in flat cable	25mm × 0.2mm
Steel cross section, mm^2	893.5
Conduit inner corner radius, mm	8

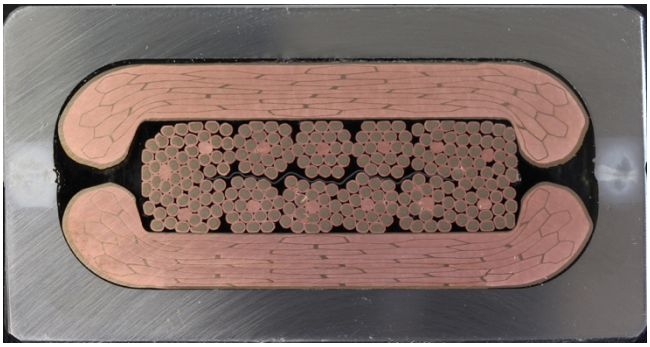

Fig. 1. Cross section of the RW2 prototype conductor with full mixed matrix stabilizer.

II. THE RW2 CONDUCTOR

For the investigations on bending tolerance the second RW prototype conductor, RW2, is selected, which was assembled at SPC in 2018. A summary of the key data is gathered in Table I. A cross section is shown in Fig.1. Among the various layouts of RW2, the "RW2 full mixed matrix" has the best DC performance thanks to the transverse compression applied during assembly, see [13] for detail of the assembly procedure and test results.

The T_{cs} performance of RW2, measured in 2018 in SULTAN at 63 kA / 10.9 T, is shown in Fig.2. A total of 1000 electromagnetic (em) load cycles and four warm-up/cool-down cycles, WUCD, were carried out in two test campaigns. The initial T_{cs} decreases by ≈ 60 mK during the test campaign and recovers upon WUCD to the initial value or higher. The effective strain, obtained by matching the final performance with the strand scaling law, was estimated as low as -0.27%, in good agreement with the expected thermal strain [13].

III. THE BENDING AND TEST PROCEDURES

The RW2 full mixed matrix conductor section was dismantled from the SULTAN sample tested in 2018. Fiducial markers are spot welded on the jacket, spaced by 0.7 m in the central part of the conductor section. Accurate length measurements are taken before and after each bending to monitor the elongation/ shrinkage, which may occur upon plastic deformation of the steel jacket and modify the longitudinal strain for the Nb_3Sn. It is important to separate the effect of longitudinal strain change from the bending tolerance.

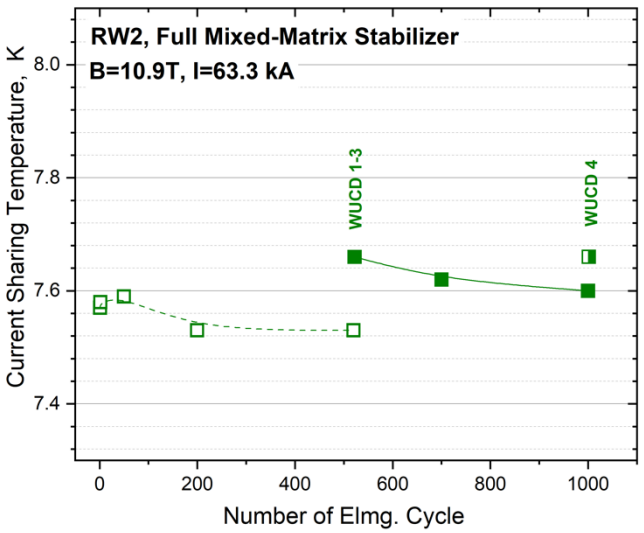

Fig. 2. The T_{cs} performance of RW2 as a function of em and thermal cycles in 2018 (no bending). The empty symbols are from the first campaign, followed by three WUCD, the second campaign (full symbols) and a final WUCD.

A total of seven test campaigns in SULTAN are planned, named B0 to B6. The first test campaign, B0, with no bending applied, is a bench mark of the tests in 2018 and provides the reference DC results to evaluate the performance change upon bending. The following six test campaigns, B1 to B6, are carried out after bending at decreasing radii.

To do the bending, the SULTAN sample is dismantled, the instrumentation is removed, the length between the fiducial markers is measured, the conductor section is bent over a machined Al former using clamps to force it to the desired radius, the conductor is straightened, the length is measured again, the instrumentation is applied and the conductor is assembled again into a SULTAN sample. Six sets of Al formers are prepared with different radii. The procedure of bending is shown in Fig.3. The instrumentation scheme is the same as for all the RW prototype samples, see [12].

A summary of the bending data is gathered in Table II, including the radii of the Al formers, the corresponding bending strain on the 10.8 mm thick cable, the length measurement before and after bending and the corresponding longitudinal strain relative to the initial non-bent conductor. The bending strain is calculated as the cable half thickness (5.4 mm) divided by the radius of the Al frame, R, plus half conductor height, 16 mm,

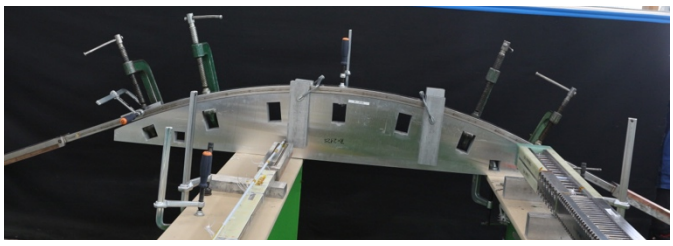

Fig. 3. Bending of the conductor section over the machined Al former at R = 1417 mm.

TABLE II

BENDING AND STRAIN DATA

Test campaign	Former radius	Bending strain	Length before bending	Length after bending	Long. Strain wrt B0
B0	-	-	699.714 mm	699.714 mm	-
B1	8300 mm	±0.065%	699.714 mm	699.533 mm	-0.026%
B2	4514 mm	±0.12%	699.552 mm	699.373 mm	-0.049%
B3	2125 mm	±0.25%	699.39 mm	699.468 mm	-0.035%
B4	1417 mm	±0.38%	699.449 mm	699.459 mm	-0.036%
B5	1155 mm	±0.46%	699.431 mm	699.305 mm	-0.058%
B6	1000 mm	±0.53%	699.269 mm	699.542 mm	-0.025%

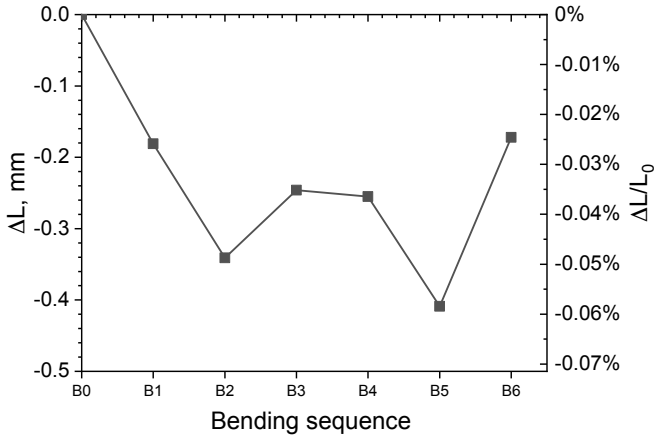

Fig. 4. Length change of the conductor at successive bending steps, measured at the fiducial markers attached to the steel conduit. Left is the absolute length change over 0.7 m, right is the percentage change, i.e. the conduit longitudinal strain.

$$\varepsilon = \pm 5.4/(R+16)$$

The flat cable is considered as a solid body. This is a rather conservative assumption, as in fact some sliding occurs in the strand bundle upon bending.

The assembly of the machined steel profiles is performed by manual TIG longitudinal welding [12], which can be associated to large residual stress in austenitic stainless steels. The ensuing bending operations cause a small (but noticeable) shrinkage. From Table II, there is also a very small length change from "after bending" to next "before bending", due to the sample assembly, cool-down for test and warm-up. Those changes, either positive or negative, are much smaller compared to the change of length due to bending. In Fig.4 the length measured after each bending is shown with respect to the original length.

The DC test program is strictly identical from B0 to B6. It includes the instrumentation check, two identical T_{cs} runs at 63 kA and 10.9 T background field, 50 electromagnetic cycles (0 to 63 kA at 10.9 T) and a final T_{cs} run.

IV. DC RESULTS AND DISCUSSION

The assessment of the bending tolerance is based on the T_{cs} results at 10 μV/m. The operating current and the peak magnetic field are close to the actual operating conditions for DEMO TF coils [16].

The results are summarized in Fig. 5. In all test campaigns, including B0 before any bending, the initial T_{cs} is systematically lower by ≈60 mK compared to the final T_{cs}, after 50 em cycles.

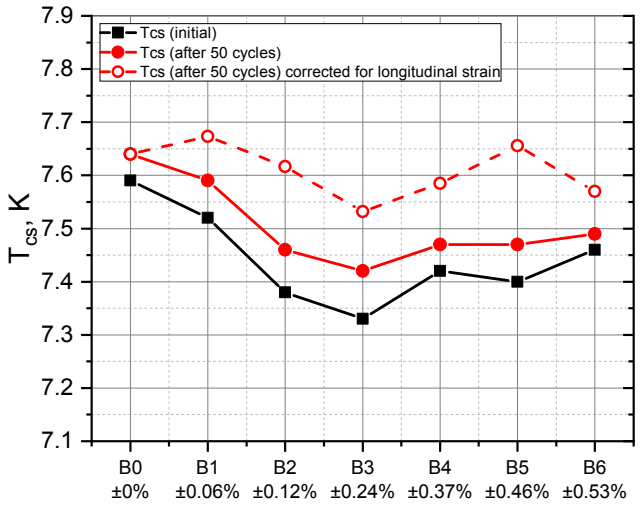

Fig. 5. T_{cs} performance at 63.3 kA / 10.9 T background field through the seven test campaigns with different applied bending strain. The empty symbols show the T_{cs} after correction for the longitudinal strain in B1-B6.

This behavior is in contrast with the 2018 test campaigns, where the initial value was higher than that after the em loading, see Fig.2. The B0 results are in good agreement with the 2018 results: the range of T_{cs} in 2018 was 7.54 – 7.66 K, compared to 7.59 – 7.64 K in B0.

There is a correlation between the T_{cs} performance from Fig.5 and the longitudinal strain from Fig.4. From the scaling law for the strand used in RW2 [13], the dependence of the current sharing temperature as a function of the longitudinal strain, $T_{cs}(\varepsilon)$, is calculated at the operating conditions, i.e. 63.3 kA, ≈ 11. 5 T (effective field at a background field of 10.9 T) and ε = -0.3%. Over a small range of strain, $T_{cs}(\varepsilon)$ is linear, with $\Delta T_{cs}/\Delta \varepsilon$ = 4.8 K, where ε is expressed in %.

To separate the effect of longitudinal strain from the bending

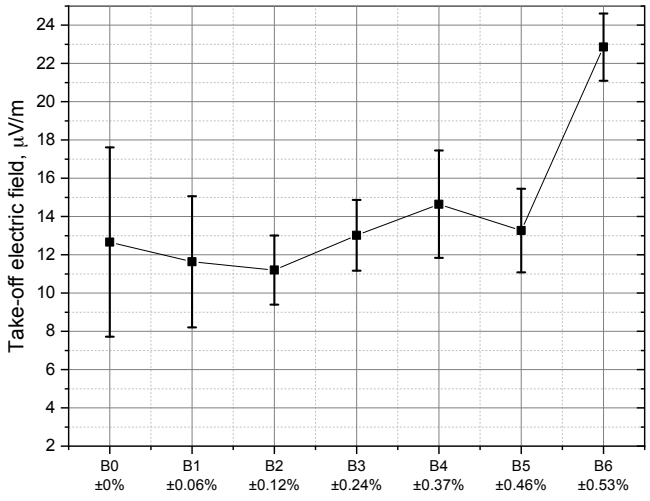

Fig. 6. Summary of the take-off electric field. The symbols are the average of three runs in the same test campaign. The bar is the range of the three T_{cs} runs in each campaign.

strain, the results of the test campaign B1 to B6 are corrected for the change of conductor length, i.e. for the longitudinal strain, see the open symbols in Fig.5. To do the correction, we assume that 2/3 of the axial strain measured on the jacket is actually transferred to the strands in the twisted bundle with low void fraction [17, 18].

After correction for the change of longitudinal strain, the T_{cs} results are all close together suggesting that there is no significant bending degradation for the RW2 cable at least up to ± 0.53% bending strain. The residual scattering of the T_{cs} is in the range of ± 50 mK with respect to the B0 result.

In Nb_3Sn CICC, the broadening of the superconducting transition and the increase of the take-off electric field are evidence of performance degradation. The take-off electric field in RW2 remains substantially constant through B1-B5, see Fig.6, and has a clear increase at B6. We understand the increase of the take-off electric field at B6 as the inception of irreversible degradation.

The superconducting transition is reported (without any correction) in Fig.7, confirming that the transition index remains constant. The shift between the curves corresponds to the variation of longitudinal strain (shrinkage upon bending).

V. Conclusion

The bending tolerance for the RW, non-soldered, flat cable developed at SPC is larger than assumed in the tentative design criteria (±0.3% retaining the flat cable as a solid body). The test on RW2 conductor suggests no T_{cs} degradation up to ±0.53% bending, but the take-off electric field starts increasing at the last bending step, suggesting an inception of irreversible degradation. Based on this finding we suggest updating to ±0.5% the limit for handling strain. In terms of design of RW conductors, the cable thickness can be increased and/or the minimum bending radius for transportation can be decreased.

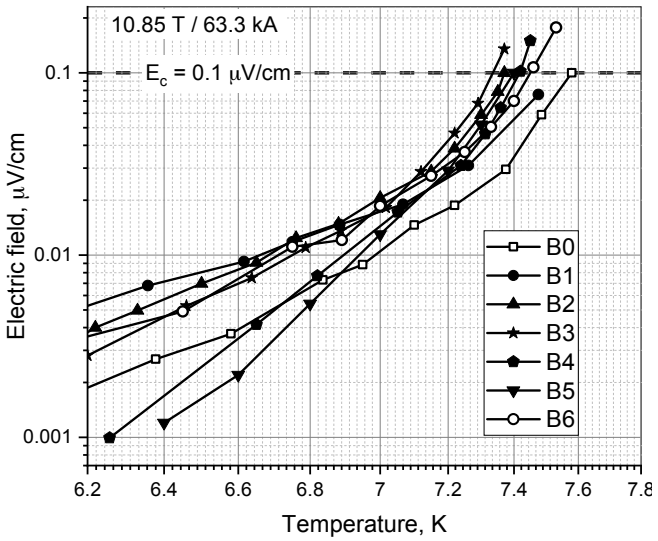

Fig. 7. Electric field vs. temperature (T_{cs} transition) for the final run of all the seven campaigns. No correction applied. The open symbols are used to highlight the first and final test campaign.

The prediction of the longitudinal strain in Nb_3Sn is usually done by calculation of the thermal strain and the application of the operating loads. Actually a small but non-negligible impact is due to the length change of the steel jacket upon bending, leading to additional compressive strain for Nb_3Sn. Such change of length may be related to a partial relief of the residual stress induced during the longitudinal welding of the jacketing operation. It is recommended to verify the length change upon bending for the actual state of the steel.

Acknowledgment

The authors are indebted with the SPC workshop and SULTAN operation team for their skilled and dedicated support.

References

[1] P. Bruzzone *et al.*, “LTS and HTS High Current Conductor Development for DEMO”, *Fusion Eng. Des.*, Vol. 96–97, pp 77-82, October 2015.

[2] N. Mitchell *et al.*, “Superconductors for fusion: a roadmap” section “12. Advances in React-and-Wind Nb_3Sn coils for fusion”, *Supercond. Sci. Technol*. 34 (2021) 103001.

[3] ITER Final Design Report 2001: DRG1 Annex “Magnet Superconducting and electrical Design Criteria”, IAEA Vienna 2001.

[4] K. Kim *et al.*, “Status of the KSTAR superconducting magnet system development”, *Nucl. Fusion* 45, 783, 2005

[5] H. Murakami *et al*., "Completion of Central Solenoid for JT-60SA," *IEEE Trans. Appl. Supercond.*, vol. 31, no. 5, pp. 1-5, Aug. 2021.

[6] T. A. Kozman *et al*., “Magnets for the mirror fusion test facility: testing of the first Yin-Yang and the design and development of the other magnets”, *IEEE Trans. Magn.,* 19, 859, 1983.

[7] E. N. Bondarchuk, *et al*., “Tokamak-15 electromagnetic system. Design and test results”, *Plasma Devices Oper.*, 2, 1, 1992.

[8] B. Jakob, G. Pasztor, R.G. Schindler, “Fabrication of high current Nb_3Sn forced flow conductors and coils for the SULTAN III test facility”, *Fusion Technol. 1992,* 872 (Elsevier 1993)

[9] Y. Takahashi *et al.,* “Experimental results of the Nb_3Sn demo poloidal coil (DPC-EX)”, *Cryogenics* 31, 640, 1991.

[10] Y. Nakamura, A. Nagao, N. Hiraki and S. Itoh, “Reliable and stable operation of the high field superconducting tokamak TRIAM-1M”, *Proc. Magnet Technology Conference MT-11*, 767 Tsukuba, 1990 (Elsevier).

[11] B. A. Smith *et al*., "Design, fabrication and test of the react and wind, Nb3Sn, LDX floating coil," *IEEE Trans. Appl. Supercond.*, vol. 11, no. 1, pp. 2010-2013, March 2001.

[12] P. Bruzzone *et al.*, “Design, Manufacture and Test of a 82 kA React&Wind TF Conductor for DEMO”, *IEEE Trans. Appl. Supercond*., 26, 4801805, 2016.

[13] K. Sedlak *et al*., "DC Test Results of the DEMO TF React&Wind Conductor Prototype No. 2," *IEEE Trans. Appl. Supercond*, vol. 29, 4801005, 2019.

[14] P. Bruzzone, K. Sedlak, B. Stepanov, M. Kumar and V. D'Auria, "A New Cabled Stabilizer for the Nb_3Sn React&Wind DEMO Conductor Prototype," *IEEE Trans. Appl. Supercond*, vol. 31, 4802505, 2021.

[15] F. Demattè *et al*., "Preliminary Design of a High Current R&W TF Coil Conductor for the EU DEMO," *IEEE Trans. Appl. Supercond*, vol. 32, 4202504, 2022.

[16] K. Sedlak *et al*., “Design and R&D for the DEMO Toroidal Field Coils Based on Nb_3Sn React and Wind Method”, *IEEE Trans. Appl. Supercond*. vol. 27, 4800105, 2017.

[17] H. Bajas, “Numerical simulation of the mechanical behavior of the ITER cable-in-conduit conductors”, PhD thesis, Ecole Centrale Paris, 2011.

[18] N. Mitchell, “Operating strain effects in Nb_3Sn cable-in-conduit conductors”, *Supercond. Sci. Technol*. 18 (2005) S396.